energies

MDPI

Article

A Fourth Order Numerical Scheme for Unsteady Mixed Convection Boundary Layer Flow: A Comparative Computational Study

Yasir Nawaz [1,2], Muhammad Shoaib Arif [1,3,*], Wasfi Shatanawi [3,4,5] and Muhammad Usman Ashraf [2]

1 Department of Mathematics, Air University Islamabad, PAF Complex E-9, Islamabad 44000, Pakistan; yasir.nawaz.v@nu.edu.pk
2 Department of Sciences and Humanities, National University of Computer and Emerging Sciences, Islamabad 44000, Pakistan; usman.ashraf@nu.edu.pk
3 Department of Mathematics and Sciences, College of Humanities and Sciences, Prince Sultan University, Riyadh 11586, Saudi Arabia; wshatanawi@psu.edu.sa
4 Department of Medical Research, China Medical University Hospital, China Medical University, Taichung 40402, Taiwan
5 Department of Mathematics, Faculty of Science, The Hashemite University, P.O. Box 330127, Zarqa 13133, Jordan
* Correspondence: shoaib.arif@mail.au.edu.pk or marif@psu.edu.sa

Abstract: In this paper, a three-stage fourth-order numerical scheme is proposed. The first and second stages of the proposed scheme are explicit, whereas the third stage is implicit. A fourth-order compact scheme is considered to discretize space-involved terms. The stability of the fourth-order scheme in space and time is checked using the von Neumann stability criterion for the scalar case. The stability region obtained by the scheme is more than the one given by explicit Runge–Kutta methods. The convergence conditions are found for the system of partial differential equations, which are non-dimensional equations of heat transfer of Stokes first and second problems. The comparison of the proposed scheme is made with the existing Crank–Nicolson scheme. From this comparison, it can be concluded that the proposed scheme converges faster than the Crank–Nicolson scheme. It also produces less relative error than the Crank–Nicolson method for time-dependent problems.

Keywords: three-stage scheme; fourth-order scheme; stability; convergence; mixed convection

check for updates

Citation: Nawaz, Y.; Arif, M.S.; Shatanawi, W.; Ashraf, M.U. A Fourth Order Numerical Scheme for Unsteady Mixed Convection Boundary Layer Flow: A Comparative Computational Study. *Energies* **2022**, *15*, 910. https://doi.org/10.3390/en15030910

Academic Editors: Magdalena Piasecka and Krzysztof Dutkowski

Received: 15 December 2021
Accepted: 17 January 2022
Published: 27 January 2022

Publisher's Note: MDPI stays neutral with regard to jurisdictional claims in published maps and institutional affiliations.

Copyright: © 2022 by the authors. Licensee MDPI, Basel, Switzerland. This article is an open access article distributed under the terms and conditions of the Creative Commons Attribution (CC BY) license (https://creativecommons.org/licenses/by/4.0/).

1. Introduction

Numerical methods play a vital role in solving mathematical models of physical phenomena. The mathematical models for fluid flow and heat transfer must be solved exactly or approximately using numerical methods. In the literature, several numerical approaches have been developed that involve two or more steps. These methods are called multi-step methods. The main advantage of using multi-step methods is their use for one stage, and so the solutions to the problems can be obtained in one loop. Still, it has a drawback of using any scheme on a first-time level or choosing one or more initial estimates to initialize the multi-step scheme.

On the other hand, Runge–Kutta methods have been constructed on different stages, and so these methods may consume more time than multi-step methods. These methods have the main advantage of providing greater stability region and do not require any other scheme on a first-time level. Mostly implicit methods provide greater stability regions than explicit methods, and some are unconditionally stable.

Compact schemes can be constructed to get the high accuracy of the solution. In [1], a sixth-order compact scheme has been constructed to solve Poisson equations with fixed or Dirichlet boundary conditions. The sixth order has been proved numerically and

analytically, and it was shown that the sixth order scheme outperformed the existing fourth-order scheme. Two schemes were proposed in [2] for solving a Dirac equation with the periodic boundary conditions. The vectored forms of schemes were analyzed by finding convergence and conservative properties. In the literature, numerical schemes exist for solving problems having shock waves. In [3], a nested multi-resolution finite-difference fifth-order WENO scheme has been given. The scheme produced less error when it was compared with the classical fifth-order WENO scheme for the smooth region. The scheme switched to third and first orders near the discontinuous and strongly discontinuous regions. The scheme produced smaller numerical dissipation without using any dissipation preserving method. A higher-order compact scheme [4] was given for stratified rotating flows. The scheme was validated with analytical solutions. The code was useful to reduce the huge execution times. The Symplectic scheme has been proposed in [5], with three free parameters covering the implicit midpoint methods, symplectic Euler, and Stormer–Verlet methods. Moreover, second-order symplectic and symmetric symplectic schemes were obtained with two free parameters and a free parameter, respectively. A compact scheme was developed in [6] for second-order Schrodinger and parabolic partial differential equations using Dirichlet and Neumann boundary conditions and which had a smaller error and high order than the classical implicit scheme. The non-oscillatory behavior of numerical schemes is not the only requirement in hyperbolic conservation laws, but also it is required for singular perturbation problems. In [7], a Gaussian radial basis functions finite difference method was given to achieve a non-oscillatory solution using the finite difference method for any degree of resolution. The non-oscillatory solution of singular perturbation problems was obtained even with the small number of grid points. A compact nonlinear scheme [8] is given to solve the nonlinear Schrodinger equation on an unbounded domain. First, a method is applied to reduce the problem from unbounded domain to initial boundary value problem on a bounded domain, and then it is solved by the proposed method. One of the features of the scheme was to avoid time-consuming iterations. A class of second-order in time and fourth-order in space compact schemes [9] has been given to solve the Burgers' equations. In addition to this, linear stability analysis was also carried out to prove that the scheme is conditionally stable. A fourth-order gas kinetic scheme [10] is based on two-stage time discretizing and Hermite WENO reconstruction to solve compressible Euler equations and Navier–Stokes equations. Comparing the DG method, both used the same stencil, but the gas–kinetic scheme used two stages of the time integration scheme. In contrast, the DG method utilized four stages of the time integration method. The fourth-order compact difference scheme has been proposed in [9] to solve Burgers' equations. The scheme was fourth order in space and second-order in time, and linear stability analysis was also carried out. It was found that the scheme is conditionally stable. Since it was built on three grid points, the Thomas algorithm was considered for solving the tridiagonal system. Further, the scheme was also applied for solving two and three-dimensional Burgers' equations. More work on the compact scheme can be seen in [10,11]. In the literature, implicit–explicit schemes have been proposed to solve differential equations numerically, and accelerated implicit–explicit schemes [12] have been proposed to solve stiff problems. The problem can be split into non-stiff and stiff constituent parts which were allowed by these schemes. The research work on the Runge–Kutta method can be seen in [13], in which order conditions have been found for delay differential equations. Up to order five, the stiff order conditions have been found. The exponential Runge–Kutta methods have been given [14] for delay differential equations which are semilinear parabolic. Conditions for DN-stability and stiff convergence have been examined, with these characteristics being offered in the context of the analytic semigroup framework. Up to order four, the stiff convergence order conditions have been derived. A third-order in time adaptive order Runge–Kutta method and finite volume in space for advection–diffusion equations have been implemented in [15]. The spatial derivatives have essentially been discretized by a weighted non-oscillatory (WENO) scheme. To reduce spurious oscillations, spatially partitioned Runge–Kutta methods have been employed. The

structure-preserving family of exponential Runge–Kutta methods has been developed [16]. These methods were combined with the scalar auxiliary variable approach. A modified version of the explicit two-stage Runge–Kutta scheme of four, five, and six order has been derived in [17] to test a 2D cylinder and a 3D Taylor–Green vortex problem. It was claimed that proposed modified schemes were 25% faster than the Low-Storage Runge–Kutta method of the same order. A class of Maximum principal preserving integrators for the Allen–Cahn equation has been designed and analyzed [18]. The space discretization was performed by applying the second-order finite difference scheme. A fully discrete scheme was obtained by applying Lawson transformation and the Runge-Kutta scheme for discretizing time. Since some implicit compact numerical schemes do not converge for the convection-diffusion type equations, an explicit compact scheme has been proposed in [19] to overcome this deficiency of implicit scheme. The scheme was applied for the particular type of convection-diffusion problems and provided fourth-order accuracy in space and second-order accuracy in time.

2. Numerical Scheme

There exist numerous numerical schemes for solving time-dependent partial differential equations. The advantages and shortcomings of using multi-step and multi-stages or Runge–Kutta types of schemes have been mentioned earlier. For a better understanding, the performance of any scheme is its compared results with the existing known scheme on the different types of problems. For spatial variables, a compact scheme is chosen. The compact scheme of fourth order uses fewer grid points than the classical standard difference scheme of the same order. So, the fourth-order accurate solution in time and space can be obtained for parabolic equations.

To construct a numerical scheme for solving a time-dependent partial differential equation, consider the differential equation of the form

$$\frac{\partial u}{\partial t} = \frac{\partial^2 u}{\partial x^2} \tag{1}$$

For the first stage of the proposed scheme, consider the discretization of Equation (1) in a form

$$\overline{u}_i^{n+1} = u_i^n + \Delta t \left(\frac{\partial u}{\partial t} \right)_i^n \tag{2}$$

where $\overline{u}_i^{n+1}$ is an unknown time level at the first stage of the scheme. Let the second stage of the proposed scheme be given by

$$\overline{\overline{u}}_i^{n+1} = \frac{1}{2} \left[u_i^n + \overline{u}_i^{n+1} + \Delta t \left(\frac{\partial \overline{u}}{\partial t} \right)_i^{n+1} \right] \tag{3}$$

It should be observed that the first and second stages of the proposed schemes are explicit. For starting the third stage of the proposed scheme, consider the difference scheme with unknowns given as

$$u_i^{n+1} = u_i^n + \Delta t \left\{ a \left(\frac{\partial \overline{u}}{\partial t} \right)_i^{n+1} + b \left(\frac{\partial \overline{\overline{u}}}{\partial t} \right)_i^{n+1} + c \left(\frac{\partial u}{\partial t} \right)_i^{n+1} + c_1 \left(\frac{\partial u}{\partial t} \right)_i^{n} \right\} \tag{4}$$

Substituting first and second stages (2) and (3) into stage three (4) and Taylor series expansion for $\left(\frac{\partial u}{\partial t} \right)_i^{n+1}$, it is obtained

$$u_i^{n+1} = u_i^n + \Delta t \left\{ \begin{array}{c} a\left(\frac{\partial u}{\partial t}\right)_i^n + a\Delta t\left(\frac{\partial^2 u}{\partial t^2}\right)_i^n + \frac{b}{2}\left(\frac{\partial u}{\partial t}\right)_i^n + \frac{b}{2}\Delta t\left(\frac{\partial^2 u}{\partial t^2}\right)_i^n + \\ \frac{b}{2}(\Delta t)^2\left(\frac{\partial^3 u}{\partial t^3}\right)_i^n + c\left(\frac{\partial u}{\partial t}\right)_i^n + c\Delta t\left(\frac{\partial^2 u}{\partial t^2}\right)_i^n + \\ \frac{c}{2}(\Delta t)^2\left(\frac{\partial^3 u}{\partial t^3}\right)_i^n + \frac{c}{6}(\Delta t)^3\left(\frac{\partial^4 u}{\partial t^4}\right)_i^n + c_1\left(\frac{\partial u}{\partial t}\right)_i^n \end{array} \right\} \tag{5}$$

Expanding u_i^{n+1} using the Taylor series and comparing coefficients on both sides of Equation (5) it is obtained

$$\left. \begin{array}{c} 1 = a + b + c + c_1 \\ \frac{1}{2} = a + b + c \\ \frac{1}{6} = \frac{b}{2} + c \\ \frac{1}{24} = \frac{c}{6} \end{array} \right\} \tag{6}$$

Solving Equation (6) gives the values of a, b, c and c_1 as

$$a = \frac{1}{6},\ b = \frac{1}{12},\ c = \frac{1}{4},\ c_1 = \frac{1}{2} \tag{7}$$

Thus, the third implicit stage of the proposed scheme is expressed as

$$u_i^{n+1} = u_i^n + \frac{\Delta t}{12}\left\{ 2\left(\frac{\partial \overline{u}}{\partial t}\right)_i^{n+1} + \left(\frac{\partial \overline{\overline{u}}}{\partial t}\right)_i^{n+1} + 3\left(\frac{\partial u}{\partial t}\right)_i^{n+1} + 6\left(\frac{\partial u}{\partial t}\right)_i^{n} \right\} \tag{8}$$

The proposed approach discretizes only the time variable; any scheme can be used to discretize the space variable. In the present contribution, a compact fourth-order scheme is chosen. For this reason, consider the Taylor series expansions for u_{i+1}^n and u_{i-1}^n as

$$\left. \begin{array}{l} u_{i+1}^n = u_i^n + \Delta x \left(\frac{\partial u}{\partial x}\right)_i^n + \frac{(\Delta x)^2}{2}\left(\frac{\partial^2 u}{\partial x^2}\right)_i^n + \frac{(\Delta x)^3}{6}\left(\frac{\partial^3 u}{\partial x^3}\right)_i^n + \frac{(\Delta x)^4}{24}\left(\frac{\partial^4 u}{\partial x^4}\right)_i^n \\ u_{i-1}^n = u_i^n - \Delta x \left(\frac{\partial u}{\partial x}\right)_i^n + \frac{(\Delta x)^2}{2}\left(\frac{\partial^2 u}{\partial x^2}\right)_i^n - \frac{(\Delta x)^3}{6}\left(\frac{\partial^3 u}{\partial x^3}\right)_i^n + \frac{(\Delta x)^4}{24}\left(\frac{\partial^4 u}{\partial x^4}\right)_i^n \end{array} \right\} \tag{9}$$

Adding u_{i+1}^n and u_{i-1}^n yields

$$u_{i+1}^n + u_{i-1}^n = 2u_i^n + (\Delta x)^2\left(\frac{\partial^2 u}{\partial x^2}\right)_i^n + \frac{(\Delta x)^4}{12}\left(\frac{\partial^4 u}{\partial x^4}\right)_i^n + O\left((\Delta x)^4\right). \tag{10}$$

This implies,

$$\frac{u_{i+1}^n - 2u_i^n + u_{i-1}^n}{(\Delta x)^2} = \left(\frac{\partial^2 u}{\partial x^2}\right)_i^n + \frac{(\Delta x)^2}{12}\left(\frac{\partial^4 u}{\partial x^4}\right)_i^n + O\left((\Delta x)^4\right), \tag{11}$$

$$\left(\frac{\partial^2 u}{\partial x^2}\right)_i^n = \frac{u_{i+1}^n - 2u_i^n + u_{i-1}^n}{(\Delta x)^2} - \frac{(\Delta x)^2}{12}\left(\frac{\partial^4 u}{\partial x^4}\right)_i^n + O\left((\Delta x)^4\right). \tag{12}$$

The fourth derivative in Equation (12) can be found by finding the derivative of Equation (1) as,

$$\left(\frac{\partial^4 u}{\partial x^4}\right)_i^n = \frac{\partial^3 u}{\partial t \partial x^2} \tag{13}$$

Substituting Equation (13) into (12), it is obtained

$$\left(\frac{\partial u}{\partial t}\right)_i^n = \frac{u_{i+1}^n - 2u_i^n + u_{i-1}^n}{(\Delta x)^2} - \frac{(\Delta x)^2}{12}\frac{\partial^3 u}{\partial t \partial x^2}. \tag{14}$$

Equation (14) is a semi-discretized scheme that performs space discretization using a fourth-order compact scheme. This type of space discretization scheme has also been applied for partial differential equations in literature.

Equation (14) can be expressed as,

$$\left(\frac{\partial u}{\partial t}\right)_i^n = \delta_x^2 u_i^n - \frac{(\Delta x)^2}{12}\delta_x^2\left(\frac{\partial u}{\partial t}\right)_i^n, \tag{15}$$

where $\delta_x^2 u_i^n = \frac{u_{i+1}^n - 2u_i^n + u_{i-1}^n}{(\Delta x)^2}$.

Applying the first stage of the proposed scheme to Equation (15), it is obtained,

$$\overline{u}_i^{n+1} = u_i^n + \Delta t\delta_x^2 u_i^n - \Delta t\frac{(\Delta x)^2}{12}\left(\frac{\delta_x^2\overline{u}_i^{n+1} - \delta_x^2 u_i^{n+1}}{\Delta t}\right). \tag{16}$$

Applying the second stage of the proposed scheme it yields

$$\overline{\overline{u}}_i^{n+1} = \frac{1}{2}\left[u_i^n + \overline{u}_i^{n+1} + \Delta t\delta_x^2\overline{u}_i^{n+1} - \frac{(\Delta x)^2}{12}\left(\delta_x^2\overline{\overline{u}}_i^{n+1} - \delta_x^2 u_i^n\right)\right]. \tag{17}$$

The implicit and final stage of the proposed scheme for Equation (1) is given as,

$$u_i^{n+1} = u_i^n + \frac{\Delta t}{(\Delta x)^2}\left\{\begin{array}{l} a\left(\frac{\partial^2 u}{\partial x^2}\right)_i^{n+1} + b\left(\frac{\partial^2 u}{\partial x^2}\right)_i^{n+1} + \\ c\left(\frac{\partial^2 u}{\partial x^2}\right)_i^{n+1} + c_1\left(\frac{\partial^2 u}{\partial x^2}\right)_i^{n+1} \end{array}\right\} - \frac{(\Delta x)^2}{12}\left(\delta_x^2 u_i^{n+1} - \delta_x^2 u_i^n\right). \tag{18}$$

3. Algorithm

Since the proposed time-discretizing scheme comprises three stages, it requires at least four loops to compute results. Each loop for the corresponding stage of the scheme will find the solution on each grid point at a fixed time level. Since the scheme is implicit, the present strategy for solving equations is to use an iterative scheme. This iterative scheme is used for solving discretized or difference equations obtained by applying proposed scheme on considered system of partial differential equations. There will be six dependent variables due to velocity and temperature profiles and three stages of the scheme. The Matlab code is consisted on the following steps:

Step 1. Define the starting and ending points of 1D domain and also define the final time. Then, choose step sizes in space and time. Define the independent and dependent variables, choose values for dimensionless parameters. Go to the next step 2;

Step 2. Initialize the loop for the iterative scheme, define the initial conditions for each dependent variable that represents the velocity and temperature of the flow. Go to the next step 3;

Step 3. Initialize the time loop for finding the solution for each time level. In addition, Initialize the first loop for spatial direction for the first stage of the scheme. Define the boundary condition for each variable, compute the solution at each grid point, and End this spatial loop. Similarly, Initialize another loop for the second stage of the scheme and find the solution at each grid point using the same step size used for the previous loop. Then, End this second loop Initialize the loop for the third stage and find the solution at each grid point and at a particular time level. Then, End this third spatial loop for finding the final solution on each grid point. Also, end the loop for time direction. Go to the next step 4;

Step 4. Give the stopping criteria to stop the first iterative loop. If the stopping criteria are met, End this iterative loop; otherwise, go to step 3.

4. Stability Analysis

For finding the stability of the proposed scheme, the Von Neumann stability criterion is considered. According to this criterion, the dependent variables in a scheme are replaced

with other variables in time and space. Therefore, the following transformations are considered first,

$$\left.\begin{array}{c} u_i^{n+1} = E^{n+1}e^{iI\theta},\ u_{i+1}^{n} = E^{n}e^{(i+1)I\theta},\ u_{i-1}^{n} = E^{n}e^{(i-1)I\theta} \\ \overline{u}_i^{n+1} = \overline{E}^{n+1}e^{iI\theta},\ \overline{\overline{u}}_i^{n+1} = \overline{\overline{E}}^{n+1}e^{iI\theta} \end{array}\right\}, \tag{19}$$

where $I = \sqrt{-1}$. Substitution of transformation (19) into the first stage of proposed scheme (16) yields,

$$\overline{E}^{n+1}e^{iI\theta} = E^{n}e^{iI\theta} + \Delta t\left(\frac{e^{(i+1)I\theta} - e^{iI\theta} + e^{(i-1)I\theta}}{(\Delta x)^2}\right)E^{n} - \frac{1}{12}\left[\frac{e^{(i+1)I\theta} - e^{iI\theta} + e^{(i-1)I\theta}}{(\Delta x)^2}\left(E^{n+1} - E^{n}\right)\right]. \tag{20}$$

Dividing both sides of Equation (20) by $e^{iI\theta}$ results,

$$\overline{E}^{n+1} = E^{n} + \frac{\Delta t}{(\Delta x)^2}(2cos\theta - 2) - \frac{1}{12}(2cos\theta - 2)\left(E^{n+1} - E^{n}\right), \tag{21}$$

$$\overline{E}^{n+1} = \frac{\left[1 + 2d(cos\theta - 1) + \frac{1}{6}(cos\theta - 1)\right]E^{n}}{1 + \frac{1}{6}(cos\theta - 1)}. \tag{22}$$

Re-write Equation (22) in the form of,

$$\overline{E}^{n+1} = \varphi E^{n}, \tag{23}$$

where

$$\varphi = \frac{1 + 2d(cos\theta - 1) + \frac{1}{6}(cos\theta - 1)}{1 + \frac{1}{6}(cos\theta - 1)}.$$

Similarly, the relationship between $\overline{E}^{n+1}$ and E^n can be found by substituting transformations (19) to Equation (17), which results,

$$\overline{\overline{E}}^{n+1} = \varphi_1 E^{n}, \tag{24}$$

where

$$\varphi_1 = \frac{\frac{1}{2}\left[1 + \varphi + 2d(cos\theta - 1)\varphi + \frac{1}{6}(cos\theta - 1)\right]E^{n}}{1 + \frac{1}{12}(cos\theta - 1)}.$$

Similarly substituting transformations into the third stage of the proposed scheme, it is obtained,

$$E^{n+1} = \frac{1 + d(2a\varphi + 2b\varphi_1 + 2c_1)(cos\theta - 1) + \frac{1}{6}(cos\theta - 1)}{1 + \left(-2cd + \frac{1}{6}\right)(cos\theta - 1)}. \tag{25}$$

Let $cos\theta = -1$, in (25), it yields

$$E^{n+1} = \left[\frac{\frac{2}{3} + d\left(\frac{3}{2} - 3d\left(\frac{12}{5}\right)d^3\right)}{\frac{2}{3} + d}\right]E^{n} \tag{26}$$

The amplification factor and stability conditions can be expressed as

$$\left|\frac{E^{n+1}}{E^{n}}\right| \leq 1 \tag{27}$$

By drawing the graph of the third equation in (26), the stability region can be found approximately, as shown in Figure 1.

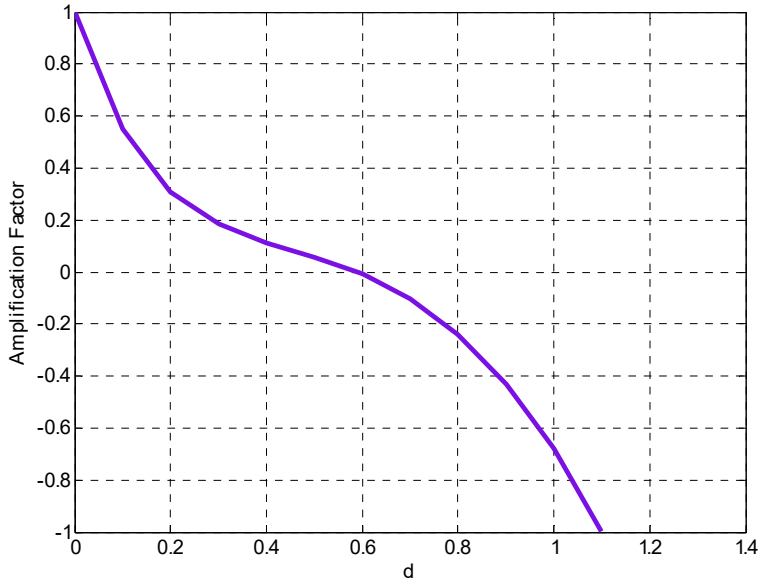

Figure 1. Amplification factor over diffusion number.

This contribution has also consisted of the mathematical model of fluid flow under heat transfer effects. The general form of the model is given as:

$$\frac{\partial u}{\partial t} = \alpha_1 \frac{\partial^2 u}{\partial x^2} + \alpha_2 u \tag{28}$$

$$\frac{\partial \theta}{\partial t} = \beta_1 \frac{\partial^2 \theta}{\partial x^2} + \beta_2 \left(\frac{\partial u}{\partial x}\right)^2 \tag{29}$$

where α_1, α_2, β_1 and β_2 are constants. System of Equations (28) and (29) can be expressed in a single equation of the form

$$\frac{\partial \boldsymbol{U}}{\partial t} = A \frac{\partial^2 \boldsymbol{U}}{\partial x^2} + B \frac{\partial \boldsymbol{U}}{\partial x} + \boldsymbol{C}\boldsymbol{U} \tag{30}$$

where $A = \begin{bmatrix} \alpha_1 & 0 \\ 0 & \beta_1 \end{bmatrix}$, $\boldsymbol{U} = \begin{bmatrix} u & \theta \end{bmatrix}^C$, $B = \begin{bmatrix} 0 & 0 \\ 2\beta_2\left(\frac{\partial u}{\partial x}\right) & 0 \end{bmatrix}$, $\boldsymbol{C} = \begin{bmatrix} \alpha_2 & 0 \\ 0 & 0 \end{bmatrix}$.

Applying first stage of the proposed scheme on Equation (30), it is obtained

$$\overline{\boldsymbol{U}}_i^{n+1} = \boldsymbol{U}_i^n + \Delta t A \delta x^2 \boldsymbol{U}_i^n - \frac{(\Delta x)^2}{12} \begin{Bmatrix} A^{-1}\frac{\partial^3 \boldsymbol{U}}{\partial x^2 \partial t} - A^{-1} B A^{-1} \frac{\partial^2 \boldsymbol{U}}{\partial x \partial t} + \\ \left(A^{-1}BA^{-1}B - A^{-1}\boldsymbol{C}\right)\frac{\partial^2 \boldsymbol{U}}{\partial x^2} \\ + A^{-1}BA^{-1}\boldsymbol{C}\frac{\partial \boldsymbol{U}}{\partial x} \end{Bmatrix} + \Delta t\, B \delta_x \boldsymbol{U}_i^n - \frac{(\Delta x)^2}{6} \begin{Bmatrix} A^{-1}\frac{\partial^2 \boldsymbol{U}}{\partial x \partial t} - \\ B\frac{\partial^2 \boldsymbol{U}}{\partial x^2} - \boldsymbol{C}\frac{\partial \boldsymbol{U}}{\partial x} \end{Bmatrix} + \boldsymbol{C}\boldsymbol{U}_i^n \tag{31}$$

where third- and fourth-order derivatives in (31) are found using Equation (30), similarly, the other two stages of the proposed scheme can be constructed.

Theorem 1. *The proposed scheme for the Equations (28) and (29) converges if it satisfies*

$$1 - \frac{1}{3}\|A^{-1}\| - \frac{1}{\Delta x}\|A_2\| \geq 0,$$

where $A_2 = \frac{(\Delta x)^2}{12} A^{-1} B A^{-1} - \frac{(\Delta x)^2}{6} A^{-1}$.

Proof. Let the error between exact and numerical scheme be denoted by $\boldsymbol{e}_i = \boldsymbol{u}_i^n - \boldsymbol{U}_i^n$. Then error equation using the first stage of the scheme is given as

$$\bar{\boldsymbol{e}}_i^{n+1} = \boldsymbol{e}_i^n + \Delta t A \delta_x^2 \boldsymbol{e}_i^n - \frac{(\Delta x)^2}{12} A^{-1}\left(\delta_x^2 \bar{\boldsymbol{e}}_i^{n+1} - \delta_x^2 \boldsymbol{e}_i^n\right) + A_2\left(\delta_x \bar{\boldsymbol{e}}_i^{n+1} - \delta_x \boldsymbol{e}_i^n\right) + A_3 \delta_x^2 \boldsymbol{e}_i^n + A_4 \delta_x \boldsymbol{e}_i^n + \boldsymbol{C}\boldsymbol{e}_i^n \tag{32}$$

where, $A_3 = -\left(A^{-1}BA^{-1}B - A^{-1}\boldsymbol{C}\right)\frac{(\Delta x)^2}{12} + \frac{(\Delta x)^2}{6}B$ and $A_4 = -\frac{(\Delta x)^2}{12}A^{-1}BA^{-1}\boldsymbol{C} + \frac{(\Delta x)^2}{6}\boldsymbol{C}$.

Applying norm on both sides of Equation (32) and using norm property, it is obtained,

$$\hat{e}^{n+1} \leq \hat{e}^n + \Delta t \|A\| \delta_x^2 \hat{e}^n + \frac{(\Delta x)^2}{12}\|A^{-1}\|\left(\delta_x^2 \hat{e}^{n+1} + \delta_x^2 \hat{e}^n\right) + \|A_2\|\left(\delta_x \hat{e}^{n+1} + \delta_x \hat{e}^n\right) + \|A_3\|\delta_x^2 \hat{e}^n + \|A_4\|\delta_x \hat{e}^n + \|\boldsymbol{C}\|\hat{e}^n \tag{33}$$

where $\hat{e}^n = \max\left(\|e_i^n,\ \bar{e}_i^n\|\right)$. From (33), the following inequality can be obtained,

$$\left(1 - \frac{1}{3}\|A^{-1}\| - \frac{1}{\Delta x}\|A_2\|\right)\hat{e}^{n+1} \leq \hat{e}^n + \frac{4\Delta t}{(\Delta x)^2}\|A\|\hat{e}^n + \frac{1}{3}\|A^{-1}\|\hat{e}^n + \frac{1}{\Delta x}\|A_2\|\hat{e}^n + \frac{4}{(\Delta x)^2}\|A_3\|\hat{e}^n + \frac{1}{\Delta x}\|A_4\|\hat{e}^n + \|\boldsymbol{C}\|\hat{e}^n \tag{34}$$

The following inequality can be obtained from (34),

$$\hat{e}^{n+1} \leq \lambda \hat{e}^n + M\left(O(\Delta t)^4, (\Delta x)^4\right), \tag{35}$$

where $\lambda = \frac{1 + \frac{4\Delta t}{(\Delta x)^2}\|A\| + \frac{1}{3}\|A^{-1}\| + \frac{1}{\Delta x}\|A_2\| + \frac{4}{(\Delta x)^2}\|A_3\| + \frac{1}{\Delta x}\|A_4\| + \|\boldsymbol{C}\|}{1 - \frac{1}{3}\|A^{-1}\| - \frac{1}{\Delta x}\|A_2\|}$.

Let, $n = 0$ in (35), it gives

$$\hat{e}^1 \leq \lambda \hat{e}^0 + M\left(O(\Delta t)^4, (\Delta x)^4\right)$$

where $\hat{e}^0 = 0$ for initial boundary condition and for $n = 1$ in (35), it is obtained

$$\hat{e}^2 \leq \lambda \hat{e}^1 + M\left(O(\Delta t)^4, (\Delta x)^4\right) \leq (1 + \lambda) M\left(O(\Delta t)^4, (\Delta x)^4\right) \tag{36}$$

If this is continued, then for any finite n,

$$\hat{e}^n \leq \left(1 + \lambda + \ldots + \lambda^{n-1}\right) M\left(O(\Delta t)^4, (\Delta x)^4\right)$$

$$\hat{e}^n \leq \frac{1 - \lambda^n}{1 - \lambda} M\left(O(\Delta t)^4, (\Delta x)^4\right)$$

Since the series $\ldots + \lambda^{n-1} + \ldots + \lambda + 1$ is a geometric series with common ratio λ, and it will converge if $|\lambda| \leq 1$. So, convergence conditions are obtained. Similarly, convergence conditions for the second and third stages can also be obtained. □

5. Applications to Engineering Problem

Example 1. *Consider a parabolic Equation (1), subject to the initial*

$$u(x, 0) = sin(x) \tag{37}$$

and boundary conditions

$$u(0, t) = 0,\ u(\pi, t) = 0 \tag{38}$$

The exact solution of the problem (1), (37), (38) is expressed as

$$u(x, t) = e^{-t} sin(x) \tag{39}$$

Figure 2 shows the comparison of relative error obtained by applying the Crank–Nicolson method with the proposed scheme. It is clearly observed that the proposed

fourth-order scheme produced less relative error than the one obtained by the second-order Crank-Nicolson method. This error can be increased and decreased by choosing different time and step sizes. Figure 3 compares the speed of the convergence of the proposed scheme and the Crank-Nicolson method. Since the proposed method is fourth-order accurate, it converges faster than the Crank-Nicolson method.

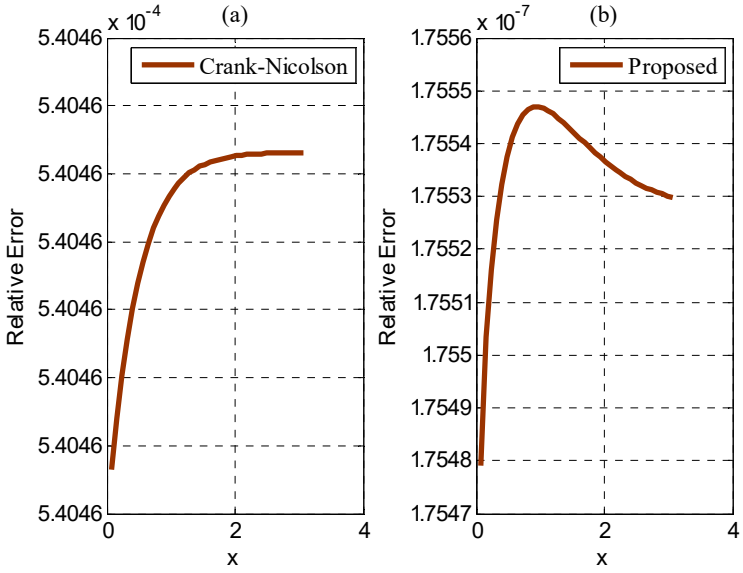

Figure 2. Comparison of two schemes over spatial coordinate using $N_x = 40$, $N_t = 520$, $L = \pi$, $t_f = 1$. (**a**) Crank–Nicolson; (**b**) Proposed.

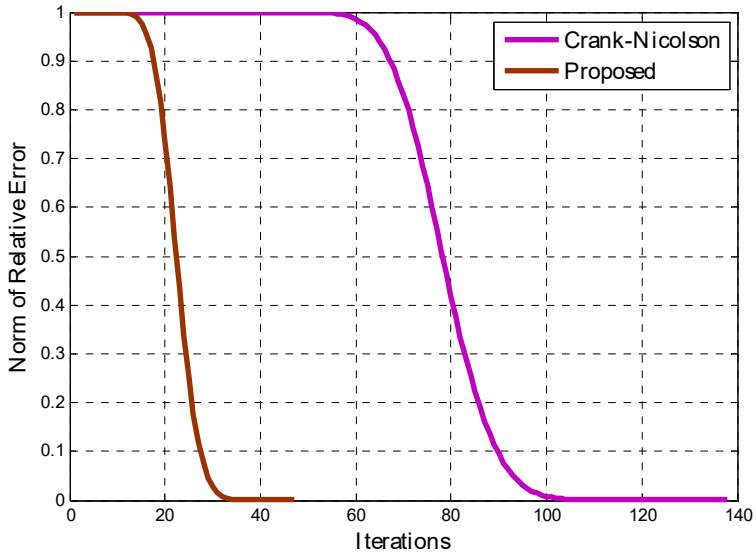

Figure 3. Comparison of speed of convergence of two schemes using $N_x = 40$, $N_t = 520$, $L = \pi$, $t_f = 1$.

Example 2. *Stokes First Problem.*

Consider unsteady, laminar, and incompressible fluid flow over the stretching sheet u_w. The sheet is infinitely long, and the flow is generated by a sudden plate movement in a positive x^*-axis direction. Let the x^*-axis be along with the plate, and y^*-axis is

perpendicular to the plate. According to Stokes assumptions, the governing equations of the flow can be expressed as

$$\frac{\partial u^*}{\partial t^*} = \nu \frac{\partial^2 u^*}{\partial y^{*2}} - \frac{\sigma B_0^2}{\rho} u^* + g\beta_T (T - T_\infty) \tag{40}$$

$$\frac{\partial T}{\partial t^*} = \alpha \frac{\partial^2 T}{\partial y^{*2}} + \frac{\mu}{\rho c_p} \left(\frac{\partial u^*}{\partial y^*} \right)^2 \tag{41}$$

subject to the initial condition

$$u^*(y^*, 0) = 0,\ T(y^*, 0) = 0, \tag{42}$$

and boundary conditions

$$\left.\begin{array}{l} u^*(y^*, t^*) = u_w,\ T(y^*, t^*) = T_w \ when\ y^* \to 0 \\ u^*(y^*, t^*) = 0,\ T(y^*, t^*) = T_\infty \ \ when\ y^* \to \infty \end{array}\right\} \tag{43}$$

The governing equations with initial and boundary conditions are dimensional, which are turned into non-dimensional equations using the transformations

$$u = \frac{u^*}{u_w},\ \theta = \frac{T - T_\infty}{T_w - T_\infty},\ t = \frac{u_w^2 t^*}{\nu},\ y = \frac{u_w y^*}{\nu} \tag{44}$$

Applying transformations (44) to Equations (40)–(43) results

$$\frac{\partial u}{\partial t} = \frac{\partial^2 u}{\partial y^2} - Mu + Gr_L \theta \tag{45}$$

$$\frac{\partial \theta}{\partial t} = \frac{1}{Pr} \frac{\partial^2 \theta}{\partial y^2} + Ec \left(\frac{\partial u}{\partial y} \right)^2 \tag{46}$$

subject to the dimensionless initial condition

$$u(y, 0) = 0,\ \theta(y, 0) = 0 \tag{47}$$

and boundary conditions are given as

$$\left.\begin{array}{l} u(y, t) = 1,\ \theta(y, t) = 1 \ when\ y \to 0 \\ u(y, t) = 0,\ \theta(y, t) = 0 \ when\ y \to \infty \end{array}\right\} \tag{48}$$

The dimensionless Equations (45)–(48) are solved by employing the proposed scheme in time and fourth-order compact scheme in space. Figure 4 shows the comparison of the speed of convergence for two schemes, showing that the proposed scheme converges faster than the Crank–Nicolson method. Figures 5 and 6 show contours for velocity and temperature profiles, respectively. Velocity and temperature are maximum at the plate $y = 0$. Then these profiles decrease from one to zero if one moves away from the plate.

Example 3. *Stokes Second Problem.*

In this problem, the sheet has behaved in the manner of a trigonometry function form. The governing equations, initial and boundary conditions are considered to be (40)–(43), except one boundary condition expressed as

$$u^*(y^*, t^*) = u_w cos(\omega t^*) \tag{49}$$

Then using the transformations [20]

$$u = \frac{u^*}{u_w},\ y = y^*\sqrt{\frac{\omega}{\nu}},\ t = \omega t^*,\ \theta = \frac{T - T_\infty}{T_w - T_\infty} \tag{50}$$

The set of dimensional Equations (40)–(43) (except one boundary condition) & (40) are reduced to Equations (45)–(48) except and including one dimensionless boundary condition given as

$$u(y,t) = cos(t) \tag{51}$$

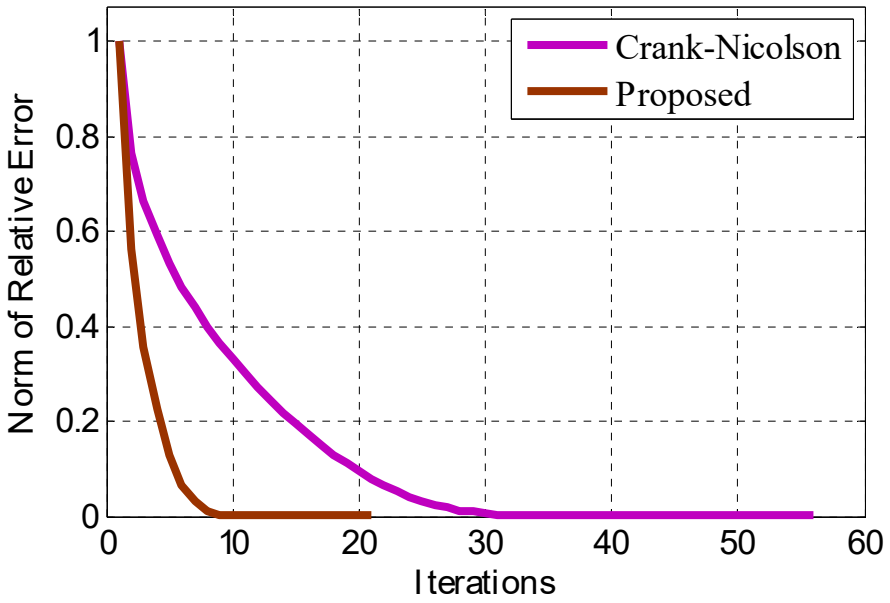

Figure 4. Comparison of speed of convergence of two schemes using $M = 0$, $N = 0$, $N_x = 40$, $N_t = 200$, $L = 17$, $t_f = 10$.

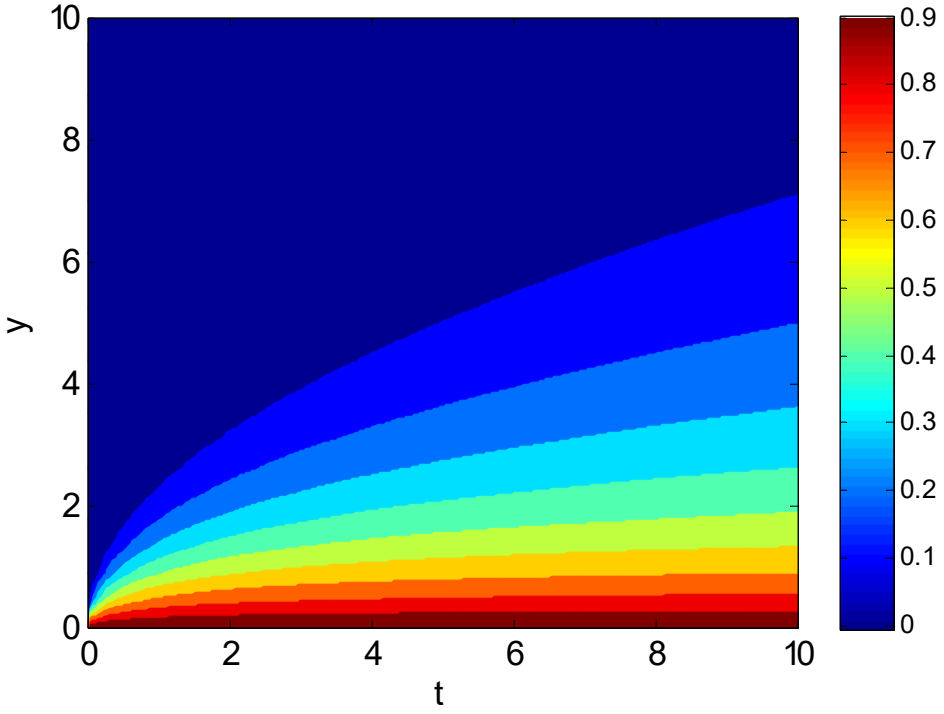

Figure 5. Contours of velocity profile.

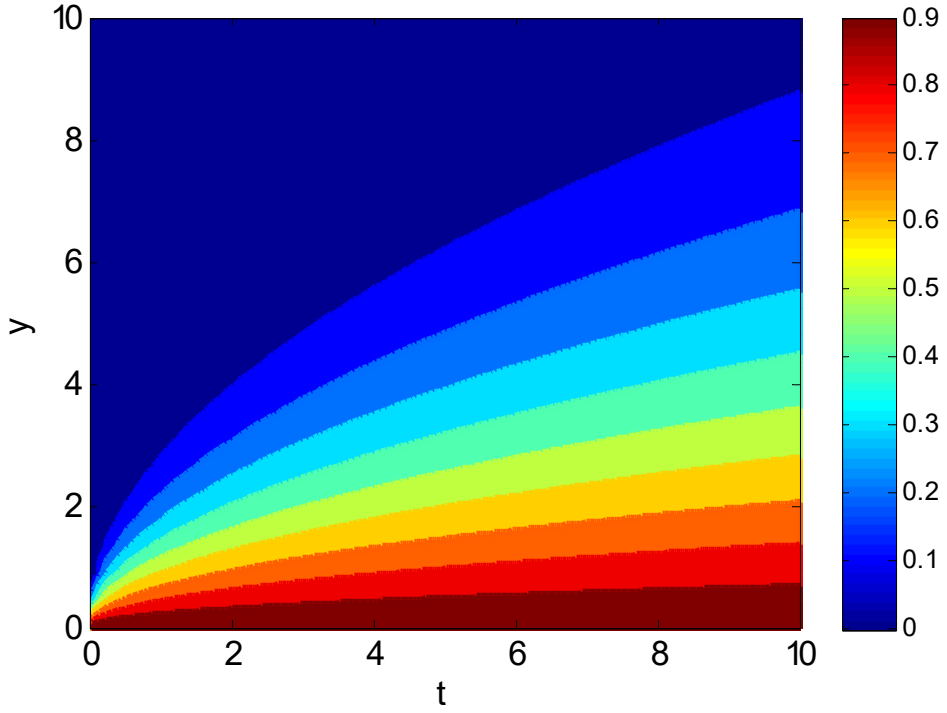

Figure 6. Contours of temperature profile.

The proposed strategy for discretizing the time variable is used to solve the set of equations for heat transport in Stokes second problem, and a compact scheme is used for spatial discretization. Figure 7 shows that the proposed scheme converges faster than the existing scheme, and also it produces a smaller norm of error than the one obtained by the Crank–Nicolson method. The contour plots are presented in Figures 8 and 9. The oscillatory behaviors of the velocity and temperature profiles can be seen in these figures.

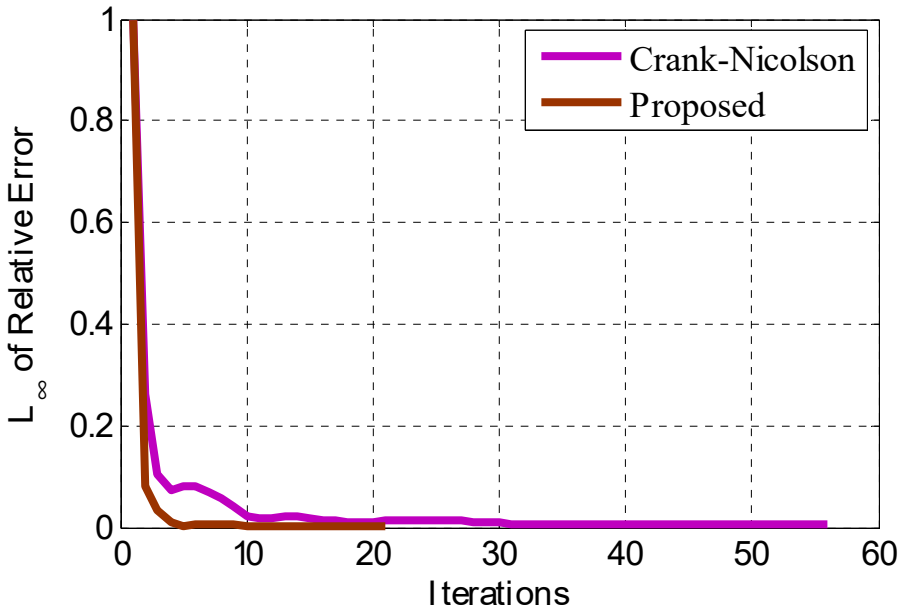

Figure 7. Comparison of speed of convergence of two schemes for Stokes second problem using $M = 0$, $N = 0$, $N_x = 40$, $N_t = 200$, $L = 17$, $t_f = 10$.

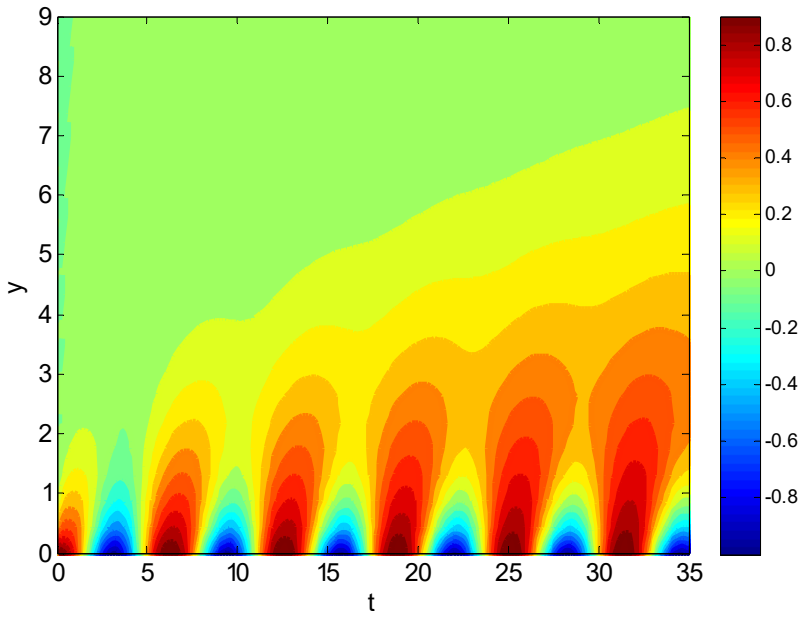

Figure 8. Contours of velocity profile for Stokes second problem.

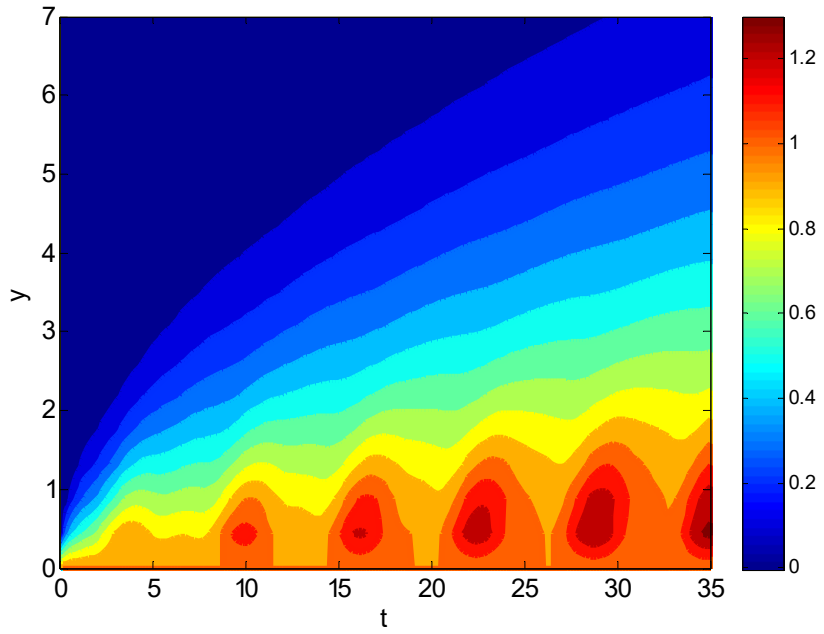

Figure 9. Contours of temperature profile for Stokes second problem.

6. Results and Discussion

The proposed numerical scheme for discretizing time variables is applied to the boundary layer flow problem. The problems of flow over the flat and oscillatory sheets are considered. These problems are associated with the energy equation, which can investigate the effect of temperature on flow. A dissipation force is also added to the energy equation, which makes the problem nonlinear. The compact scheme can be applied to solve the linear or linearized problem, and so the nonlinear term is linearized, and the proposed scheme solves the resulting linearized problem. For checking the scheme's performance, a figure is drawn that shows the stability region of the proposed scheme. This region can be compared with those given by some existing explicit schemes, and improvement in the stability region can be observed. So, the proposed scheme provides a better region of stability than some explicit schemes. For its convergence, figures for convergence of the proposed and existing

scheme are also established. Its faster convergence can be seen in the convergence plots for three kinds of problems since it stops earlier than the Crank–Nicolson method, so it converges faster than the existing second-order Crank–Nicolson scheme. Moreover, the first time-dependent problem provides less relative error than the existing Crank–Nicolson scheme. The contour plots have also been constructed that show the contours on which surface stays constant, and colors in these plots show the surface's peak or trough. Since the flow is generated due to a certain acceleration of sheet, so its effect on the adjacent layers can be seen in these figures. Additionally, when sinusoidal boundary conditions in time are chosen, it will have oscillatory effects near the time axis that can be observed in corresponding velocity and temperature contour plots.

7. Conclusions

A fourth-order numerical scheme has been constructed for solving time-dependent partial differential equations. The scheme was explicit–implicit, and it has been constructed on two-time levels. The stability of the single-equation and convergence for the system of equations has been given. The extended mathematical model for mixed convection of magnetohydrodynamics (MHD) Stokes problems has been given and solved using the proposed fourth-order scheme. Comparison with the existing Crank–Nicolson scheme showed its faster convergence. The scheme can be implemented for solving time-dependent partial differential equations. Additionally, the suggested method is straightforward to implement and may be used to a broader class of partial differential equations that are encountered in both practice and theoretical settings.

Author Contributions: Conceptualization, Y.N.; funding acquisition, W.S.; investigation, writing—original draft, methodology, Software, Formal Analysis, writing—review and editing, Y.N.; methodology, M.S.A.; project administration, W.S.; resources, W.S.; supervision, M.S.A.; visualization, W.S.; writing—review and editing, M.S.A.; Formal Analysis, M.U.A.; software, M.U.A. All authors have read and agreed to the published version of the manuscript.

Funding: The authors would like to acknowledge the support of Prince Sultan University for paying the Article Processing Charges (APC) of this publication.

Institutional Review Board Statement: Not applicable.

Informed Consent Statement: Not applicable.

Data Availability Statement: The manuscript included all required data and implementing information.

Acknowledgments: We are thankful to the anonymous referees for their valuable comments, which helped us improve the paper's quality. The second and third authors wish to express their gratitude to Prince Sultan University for facilitating the publication of this article through the research lab Theoretical and Applied Sciences Lab.

Conflicts of Interest: The authors declare no conflict of interest.

Nomenclature

u	Horizontal velocity
ν	Kinematic viscosity
σ	Electrical Conductivity
B_0	Strength of magnetic field
ρ	Density of Fluid
g	Gravity
β_T	Coefficient of Thermal Expansion
T_∞	Ambient Temperature
α	Thermal Diffusivity
c_p	Specific Heat Capacity
T_w	Wall Temperature
M	Magnetic parameter

Gr_L	Grashof number
Pr	Prandtl number
Ec	Eckert number
μ	Dynamic viscosity

References

1. Gatiso, A.H.; Belachew, M.T.; Wolle, G.A. Sixth-order compact finite difference scheme with discrete sine transform for solving Poisson equations with Dirichlet boundary conditions. *Results Appl. Math.* **2021**, *10*, 100148. [CrossRef]
2. Li, J.; Wang, T. Optimal point-wise error estimate of two conservative fourth-order compact finite difference schemes for the nonlinear Dirac equation. *Appl. Numer. Math.* **2021**, *162*, 150–170. [CrossRef]
3. Wang, Z.; Zhu, J.; Tian, L.; Zhao, N. A low dissipation finite difference nested multi-resolution WENO scheme for Euler/Navier-Stokes equations. *J. Comput. Phys.* **2021**, *429*, 110006. [CrossRef]
4. Abide, S.; Viazzo, S.; Raspo, I.; Randriamampianina, A. Higher-order compact scheme for high-performance computing of stratified rotating flows. *Comput. Fluids* **2018**, *174*, 300–310. [CrossRef]
5. Bo, Y.; Cai, W.; Wang, Y. A general symplectic scheme with three free parameters and its Applications. *Appl. Math. Lett.* **2021**, *112*, 106792. [CrossRef]
6. Gordin, V.A.; Tsymbalov, E.A. Compact difference scheme for parabolic and Schrodinger-type equations with variable coefficients. *J. Comput. Phys.* **2018**, *375*, 1451–1468. [CrossRef]
7. Gu, J.; Jung, J. Consistent, non-oscillatory RBF finite difference solutions to boundary layer problems for any degree on uniform grids. *Appl. Math. Lett.* **2020**, *115*, 106499. [CrossRef]
8. Hu, Y.; Li, H.; Jiang, Z. Efficient semi-implicit compact finite difference scheme for nonlinear Schrödinger equations on unbounded domain. *Appl. Numer. Math.* **2020**, *153*, 319–343. [CrossRef]
9. Yang, X.; Ge, Y.; Zhang, L. A class of high-order compact difference schemes for solving the Burgers equations. *Appl. Math. Comput.* **2019**, *358*, 394–417. [CrossRef]
10. Ji, X.; Pan, L.; Shyy, W.; Xu, K. A Compact fourth-order gas-kinetic scheme for the Euler and Navier–Stokes equations. *J. Comput. Phys.* **2018**, *372*, 446–472. [CrossRef]
11. Sun, Y.X.; Tian, Z.F. High-order upwind compact finite-difference lattice Boltzmann method for viscous incompressible flows. *Comput. Math. Appl.* **2020**, *80*, 1858–1872. [CrossRef]
12. Vermeire, C.; Nasab, S.H. Accelerated Implicit-Explicit Runge-Kutta Schemes for Locally Stiff Systems. *J. Comput. Phys.* **2021**, *429*, 110022. [CrossRef]
13. Fang, J.; Zhan, R. High order explicit exponential Runge–Kutta methods for semilinear delay differential equations. *J. Comput. Appl. Math.* **2021**, *388*, 113279. [CrossRef]
14. Zhao, J.; Zhan, R.; Xu, Y. Explicit exponential Runge–Kutta methods for semilinear parabolic delay differential equations. *Math. Comput. Simul.* **2020**, *178*, 366–381. [CrossRef]
15. Arbogast, T.; Huang, C.S.; Zhao, X.; King, D.N. A third order, implicit, finite volume, adaptive Runge–Kutta WENO scheme for advection–diffusion equations. *Comput. Methods Appl. Mech. Eng.* **2020**, *368*, 113155. [CrossRef]
16. Cui, J.; Xu, Z.; Wang, Y.; Jiang, C. Mass and energy preserving exponential Runge–Kutta methods for the nonlinear Schrödinger equation. *Appl. Math. Lett.* **2021**, *112*, 106770. [CrossRef]
17. Figueroa, A.; Jackiewicz, Z.; Löhner, R. Efficient two-step Runge-Kutta methods for fluid dynamics simulations. *Appl. Numer. Math.* **2021**, *159*, 1–20. [CrossRef]
18. Zhang, H.; Yan, J.; Qian, X.; Song, S. Numerical analysis and applications of explicit high order maximum principle preserving integrating factor Runge-Kutta schemes for Allen-Cahn equation. *Appl. Numer. Math.* **2021**, *161*, 372–390. [CrossRef]
19. Nawaz, Y.; Arif, M.S.; Shatanawi, W.; Nazeer, A. An Explicit Fourth-Order Compact Numerical Scheme for Heat Transfer of Boundary Layer Flow. *Energies* **2021**, *14*, 3396. [CrossRef]
20. Ishfaq, N.; Khan, W.A.; Khan, Z.H. The Stokes' second problem for nanofluids. *J. King Saud Univ.-Sci.* **2019**, *31*, 61–65. [CrossRef]